

**Effect of Ge doping concentration on the electrochemical performance of silicene anode  
for lithium-ion batteries: a first-principles study**

**Jun Song<sup>a,b</sup> \*, Mingjie Jiang<sup>a</sup>, Jodie A. Yuwono<sup>b</sup>, Sailin Liu<sup>b</sup>, Jingxiu Wang<sup>b</sup>, Qi Zhang<sup>a</sup>, Yuhui Chen<sup>a</sup>, Jun Zhang<sup>a</sup>, Xuehong Wu<sup>a</sup>, Juanfang Liu<sup>c,\*</sup>**

<sup>a</sup> *College of Energy and Power Engineering, Zhengzhou University of Light Industry, Zhengzhou 450000, Henan, China*

<sup>b</sup> *School of Chemical Engineering& Advanced Materials, The University of Adelaide, Adelaide, SA 5005, Australia*

<sup>c</sup> *School of Energy and Power Engineering, Chongqing University, Chongqing 400044, Chongqing, China*

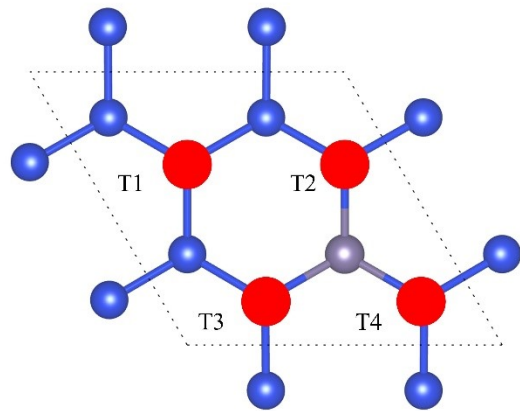


**Figure S1** Possible Li adsorption on the T sites of  $\text{Si}_7\text{Ge}_1$  on the upper surface.

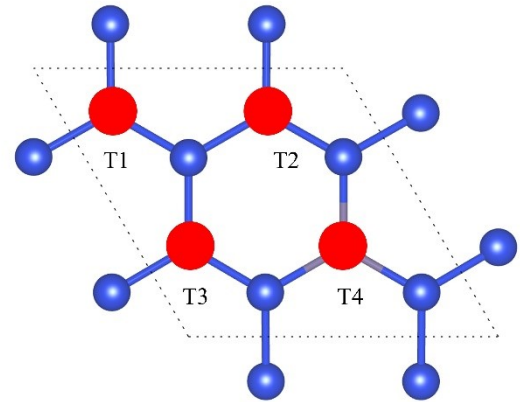


**Figure S2** Possible Li adsorption on the T sites of  $\text{Si}_7\text{Ge}_1$  on the lower surface.

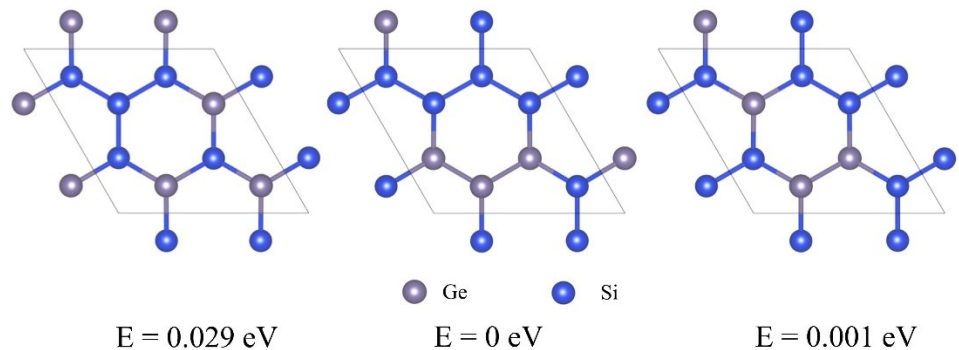


**Figure S3** Top view of three possible configurations of  $\text{Si}_5\text{Ge}_3$ .

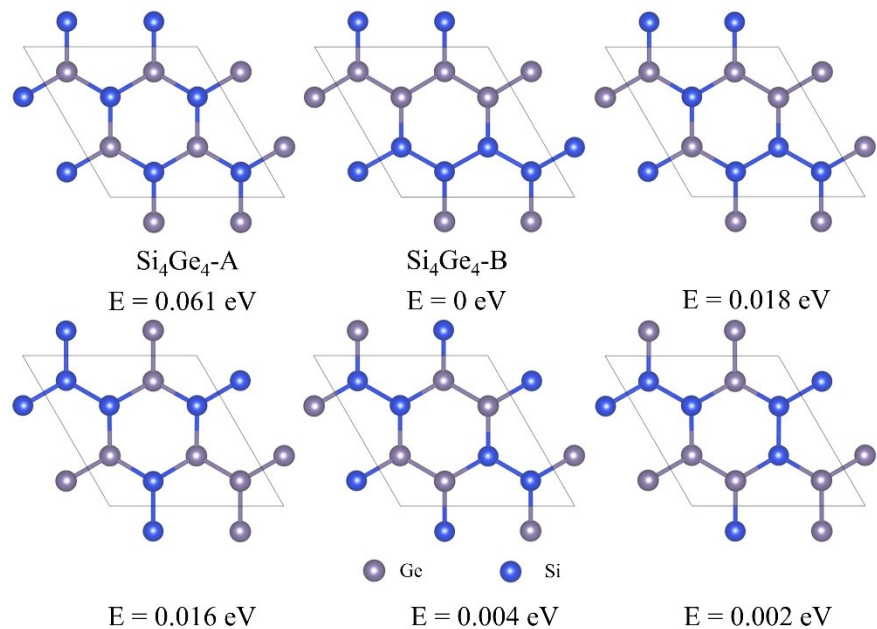


**Figure S4** Top view of six possible configurations of  $\text{Si}_4\text{Ge}_4$ .

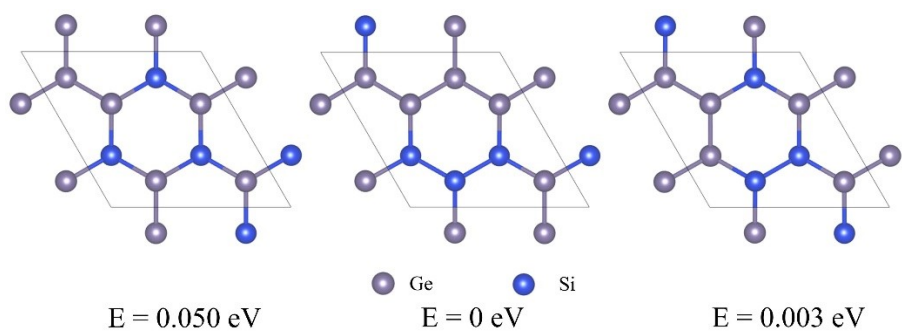


**Figure S5** Top view of three possible configurations of  $\text{Si}_3\text{Ge}_5$ .

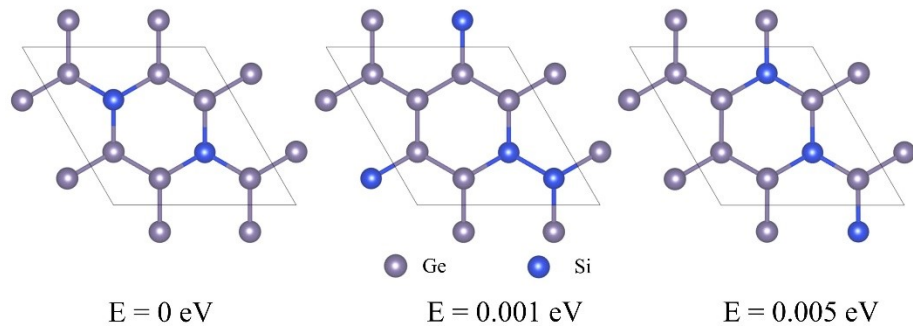


**Figure S6** Top view of three possible configurations of  $\text{Si}_2\text{Ge}_6$ .

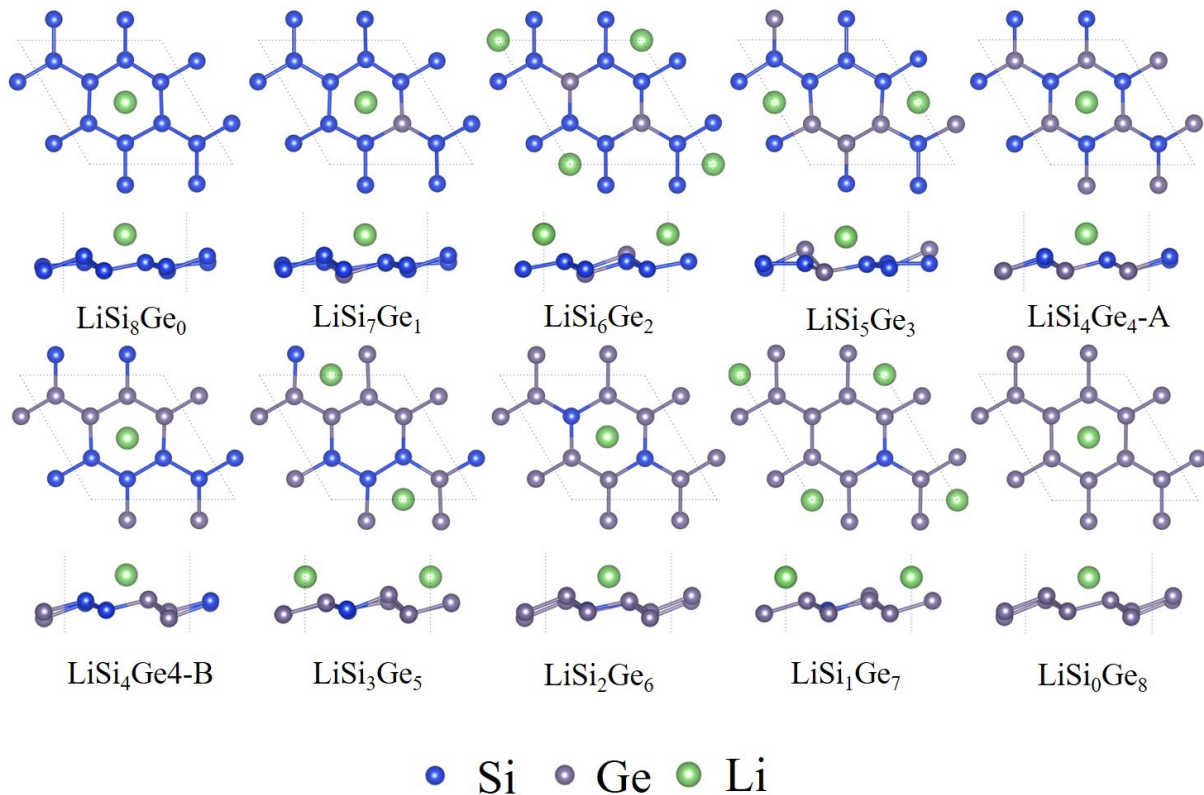


**Figure S7** Top view and side view of Li adsorption on all 2D  $\text{Si}_x\text{Ge}_y$  investigated here.

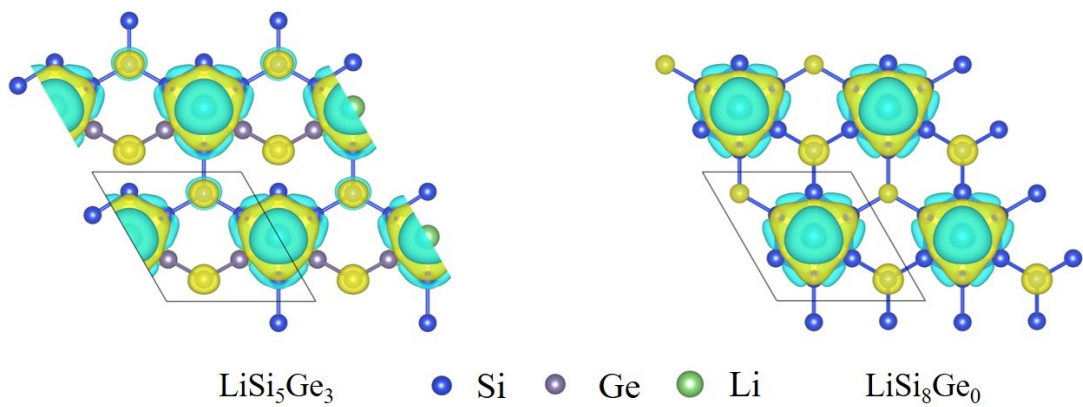


**Figure S8** Charge density difference of  $\text{LiSi}_5\text{Ge}_3$  (left) and  $\text{LiSi}_8\text{Ge}_0$  (right).

Yellow and blue color isosurfaces denotes electron loss and gain, respectively.

**Table S1** Total electronic energies without and with spin polarization correction.

Structures	Energy (eV)	Energy (eV)	$\Delta$ Energy
	ISPIN=1	ISPIN=2	
Si <sub>8</sub> Ge <sub>0</sub>	-38.7747	-38.7747	0.00%
Si <sub>7</sub> Ge <sub>1</sub>	-37.9633	-37.9633	0.00%
Si <sub>6</sub> Ge <sub>2</sub>	-37.1761	-37.1761	0.00%
Si <sub>5</sub> Ge <sub>3</sub>	-36.4005	-36.4005	0.00%
Si <sub>4</sub> Ge <sub>4</sub> -A	-35.5916	-35.5916	0.00%
Si <sub>4</sub> Ge <sub>4</sub> -B	-35.6527	-35.6527	0.00%
Si <sub>3</sub> Ge <sub>5</sub>	-34.9149	-34.9149	0.00%
Si <sub>2</sub> Ge <sub>6</sub>	-34.1827	-34.1827	0.00%
Si <sub>1</sub> Ge <sub>7</sub>	-33.5084	-33.5084	0.00%
Si <sub>0</sub> Ge <sub>8</sub>	-32.8419	-32.842	0.01%

**Table S2** Li adsorption energy on the T sites of Si<sub>7</sub>Ge<sub>1</sub> in the upper surface.

Adsorption site	Eads (eV)
T1	-1.81
T2	-1.86
T3	-1.86
T4	-1.86

**Table S3** Li adsorption energy on the T sites of Si<sub>7</sub>Ge<sub>1</sub> in the lower surface.

Adsorption site	Eads
T1	-1.84
T2	-1.84
T3	-1.84
T4	-1.97

**Table S4** Li adsorption energy on 2D  $\text{Si}_x\text{Ge}_y$ .

System	$E_{\text{ads}}$ (eV)
Silicene	-2.01
$\text{Si}_7\text{Ge}_1$	-2.04
$\text{Si}_6\text{Ge}_2$	-2.01
$\text{Si}_5\text{Ge}_3$	-2.15
$\text{Si}_4\text{Ge}_4\text{-A}$	-2.01
$\text{Si}_4\text{Ge}_4\text{-B}$	-2.00
$\text{Si}_3\text{Ge}_5$	-2.03
$\text{Si}_2\text{Ge}_6$	-2.00
$\text{Si}_1\text{Ge}_7$	-2.01
Germanene	-2.01

**Table S5** The relationship between atomic ratio used in our DFT model of 2D  $\text{Si}_y\text{Ge}_z$  and the mass ratio used in the experiment.

Atomic ratio	$\text{Si}_7\text{Ge}_1$	$\text{Si}_6\text{Ge}_2$	$\text{Si}_5\text{Ge}_3$	$\text{Si}_4\text{Ge}_4\text{-A}$	$\text{Si}_4\text{Ge}_4\text{-B}$	$\text{Si}_3\text{Ge}_5$	$\text{Si}_2\text{Ge}_6$	$\text{Si}_1\text{Ge}_7$
Mass ratio	$\text{Si}_{0.73}\text{Ge}_{0.27}$	$\text{Si}_{0.54}\text{Ge}_{0.46}$	$\text{Si}_{0.39}\text{Ge}_{0.61}$	$\text{Si}_{0.28}\text{Ge}_{0.72}$	$\text{Si}_{0.28}\text{Ge}_{0.72}$	$\text{Si}_{0.19}\text{Ge}_{0.81}$	$\text{Si}_{0.11}\text{Ge}_{0.89}$	$\text{Si}_{0.05}\text{Ge}_{0.95}$

**Table S6** Maximum storage capacity and Li migration energy barrier of 2D anode materials.

2D Materials	Theoretical capacity (mhA/g)	Energy barrier (eV)
GeS <sup>[1]</sup>	256	0.19
V <sub>2</sub> C <sup>[2]</sup>	941	0.05
Nb <sub>2</sub> C <sup>[3]</sup>	542	0.03
Mo <sub>2</sub> C <sup>[4]</sup>	526	0.04
Ti <sub>3</sub> C <sub>2</sub> <sup>[5]</sup>	319	0.07
graphite <sup>[6]</sup>	372	0.40
BC <sub>7</sub> <sup>[7]</sup>	283	1.17
g-CN <sup>[8]</sup>	813	-
BC <sub>3</sub> <sup>[9]</sup>	714	0.40
C <sub>2</sub> N <sup>[10]</sup>	672	0.03
Stanene <sup>[11]</sup>	226	0.25
TiC <sup>[12]</sup>	447	0.03
TiN <sup>[12]</sup>	433	0.27
SiS <sup>[13]</sup>	446	0.17
SiSe <sup>[13]</sup>	250	0.12
ZnP <sup>[14]</sup>	556	0.56
Antimonene <sup>[15]</sup>	208	0.34

## Reference

- [1] ZHOU Y. MX (M = Ge, Sn; X = S, Se) sheets: theoretical prediction of new promising electrode materials for Li ion batteries [J]. J Mater Chem A, 2016, 4(28): 10906-13.
- [2] HU J, XU B, OUYANG C, et al. Investigations on V2C and V2CX2 (X = F, OH) Monolayer as a Promising Anode Material for Li Ion Batteries from First-Principles Calculations [J]. J Phys Chem C, 2014, 118(42): 24274-81.
- [3] HU J, XU B, OUYANG C, et al. Investigations on Nb2C monolayer as promising anode material for Li or non-Li ion batteries from first-principles calculations [J]. RSC Adv, 2016, 6(33): 27467-74.

- [4] ÇAKI<sup>R</sup> D, SEVIK C, GüLSEREN O, et al. Mo<sub>2</sub>C as a high capacity anode material: a first-principles study [J]. *J Mater Chem A*, 2016, 4(16): 6029-35.
- [5] TANG Q, ZHOU Z, SHEN P. Are MXenes Promising Anode Materials for Li Ion Batteries? Computational Studies on Electronic Properties and Li Storage Capability of Ti<sub>3</sub>C<sub>2</sub> and Ti<sub>3</sub>C<sub>2</sub>X<sub>2</sub> (X = F, OH) Monolayer [J]. *J Am Chem Soc*, 2012, 134(40): 16909-16.
- [6] YU T, ZHANG S, LI F, et al. Stable and metallic two-dimensional TaC<sub>2</sub> as an anode material for lithium-ion battery [J]. *J Mater Chem A*, 2017, 5(35): 18698-706.
- [7] DAS D, HARDIKAR R P, HAN S S, et al. Monolayer BC<sub>2</sub>: an ultrahigh capacity anode material for Li ion batteries [J]. *Phys Chem Chem Phys*, 2017, 19(35): 24230-9.
- [8] HANKEL M, SEARLES D J. Lithium storage on carbon nitride, graphenylene and inorganic graphenylene [J]. *Phys Chem Chem Phys*, 2016, 18(21): 14205-15.
- [9] LIU Y, ARTYUKHOV V I, LIU M, et al. Feasibility of Lithium Storage on Graphene and Its Derivatives [J]. *J Phys Chem Lett*, 2013, 4(10): 1737-42.
- [10] ZHANG J, LIU G, HU H, et al. Graphene-like carbon-nitrogen materials as anode materials for Li-ion and mg-ion batteries [J]. *Appl Surf Sci*, 2019, 487: 1026-32.
- [11] MORTAZAVI B, DIANAT A, CUNIBERTI G, et al. Application of silicene, germanene and stanene for Na or Li ion storage: A theoretical investigation [J]. *Electrochim Acta*, 2016, 213: 865-70.
- [12] FAN D, LU S, GUO Y, et al. Two-Dimensional Tetragonal Titanium Carbide: a High-Capacity and High-Rate Battery Material [J]. *J Phys Chem C*, 2018, 122(27): 15118-24.
- [13] KARMAKAR S, CHOWDHURY C, DATTA A. Two-Dimensional Group IV Monochalcogenides: Anode Materials for Li-Ion Batteries [J]. *J Phys Chem C*, 2016, 120(27): 14522-30.
- [14] MORTAZAVI B, BAFEKRY A, SHAHROKHI M, et al. ZnN and ZnP as novel graphene-like materials with high Li-ion storage capacities [J]. *Materials Today Energy*, 2020, 16: 100392.
- [15] SENGUPTA A, FRAUENHEIM T. Lithium and sodium adsorption properties of monolayer antimonene [J]. *Materials Today Energy*, 2017, 5: 347-54.